EVOLUTION AND CHARACTERIZATIONS OF AURIVILLIUS BISMUTH TITANATE BY MODIFIED SOLID STATE PROCESSING

M. Shahnawaz[a], S. Khan[b], and S. Mukherjee[*,c]

[a] Department of Electronics and Communication Engineering, Heritage Institute of Technology, Kolkata-700107, India.
[b] Department of Metallurgical and Materials Engineering, Jadavpur University, Kolkata-700032, India.
[c] Department of Mechanical and Automation Engineering, Amity University Kolkata, Kolkata-700135, India.

ABSTRACT: Mild agate mortar activation followed by sintering of precursors, in resemblance to modified solid state process, was studied for synthesis of the aurivillius bismuth titanate. Hand on mill activation was carried out for eight hours followed by annealing treatment at 1000°C for 12 hours in presence of air atmosphere to obtain the proper phase. Scherrer's formula was utilized to estimate crystallite size along with planes of orientation. Crystallite size was about 65nm while prominent peaks of orientations were (-117), (006), (111), (200) and others. FESEM and TEM studies were carried to obtain the morphology and estimated grain size of the synthesized aurivillius compound. Morphological features execute the material system to be nanocrystalline in nature as estimated from grain size measurement in correspondence with XRD crystallite size estimation. FTIR analysis confirms M-O coordinations of synthesized modified perovskite (aurivillius) sample. Optical property was evaluated from UV-VIS analysis with prominent absorption spectra in the visible region. Tauc plot was used to estimate the band gap to be about 2.86eV & 2eV for both direct and indirect transitions.

Keywords: Bismuth titanate; Aurivillius; Morphology; Band gap.

تطور وتوصيفات صيغة اورفوليت لتيتنات عنصر البزموث بمعالجة معدلة للحالة الصلبة

م. شاهناواز ᵃ، س. خان ᵇ و س. موخرجي ᶜ*ᵃ

الملخص : لقد قمنا بدراسة عملية تنشيط ملاط العقيق الخفيف متبوعًا بتلبيدة معدة سالفا لتكون متشابهة مع عملية الحالة الصلبة المعدلة لتوليفة اورفوليت لتيتنات عنصرالبزموث. قمنا بعملية التنشيط هذه بالمصنع لمدة ثماني ساعات تلتها المعالجة الصلبة عند درجة حرارة 1000 مئوية لمدة 12 ساعة في وجود الهواء الجوي و ذلك للحصول على الحالة المناسبة. و قمنا باستخدام صيغة سكيرر من أجل تقدير حجم البلورات المتجهة نحو السطح. و كان حجم البلورة حوالي 65 نانومتر بينما كانت الزوايا البارزة تتجه نحو (-117) و (006) و (111) و (200) وغيرها.وتم اجراء قياسين بمجهر إلكتروني متحرك ومجهر إلكتروني ماسح و ذلك للحصول على الشكل المورفولوجي ولتقدير حجم حبيبات مركب اورفوليت. هذا و تعمل الخصائص المورفولوجية على جعل نظام المواد ذات طبيعة نانوية كما هو مقدر من قياس حجم الحبيبات بالتوافق مع تقدير جهاز قياس نسبة الأشعة السينية لحجم البلورات. وقد أكد تحليل جهاز "فورييه" لتحويل طيف الأشعة تحت الحمراء "فتير" تنسيقات (M-O) لتوليفة عينة اورفوليت المعدلة . وتم تقييم الخاصية البصرية من التحليل الطيفي فوق البنفسجي المرئي مع مراحل الامتصاص البارزة في المنطقة المرئية. و قد قمنا باستخدام مخطط "توك" لتقدير الفجوة بين 2.86eV & 2eV لكل من التحولات المباشرة وغير المباشرة.

الكلمات المفتاحية : اورفوليت البزموث تيتان ؛ المورفولوجيا؛ فجوة المراحل.

Corresponding author's e-mail: smmukherjee3@gmail.com

1. INTRODUCTION

Among the Bi-Ti-O system, bismuth titanate is one of the most important having versatile applications. Memory storage, effluent treatment, optical displays, piezoelectric transducers and photocatalysis are the domain where $Bi_4Ti_3O_{12}$ is noted to be one of the promising candidates for execution Nogueira E. André *et. al.* (2014). Intergrowth of fluorite $[Bi_2O_2]^{2+}$ and perovskite $[Bi_2Ti_3O_{10}]^{2-}$ in which Bi ions occupy twelve-coordinated sites, which were found to be the basis of the structural aspects of bismuth titanate compound Chen Zhiwu *et. al.* (2009). Generally, fluorite and perovskite can be represented as $[M_2O_2]^{2+}$ and perovskite $[A_{n-1}B_nO_{3n+1}]^{2-}$, where n is the number of BO_6 octahedra. The material has ferroelectric nature with intermediate Curie temperature of about 675°C. Such material of Bi-Ti-O system also has high fatigue endurance, and considerable electro-optic switching behavior. Bismuth titanate has the potential for application in non-volatile random access memory, high temperature piezoelectric and electro-optic devices. For fluorite $[M_2O_2]^{2+}$ (M is 8-coordinated) while the three layer member of Aurivillius phase (n=3) actually represents bismuth titanate. Pavlović Nikolina *et. al.* (2009). It is observed that Bismuth titanate has monoclinic structure at room temperature and converts to a tetragonal phase at above Curie temperature and possesses low dielectric constant, low coercive field, and a high breakdown voltage Yang Qunbao *et. al.* (2003) Quite a few process routes have been developed for the synthesis of Bismuth titanate. Most of the common process routes for synthesis are hydrolysis of metal organic salts Osamu Y *et. al.* (1991), co-precipitation Horn A. Jeffrey *et. al.* (1999), sol-gel (HaoShuang Gu *et. al.* 1998; Sedlar M *et. al.* 1996) hydrothermal (Yang Qunbao *et. al.* 2003; Shi Yanhui *et. al.* 2000), mechanochemical Ng Hwee Szu *et. al.* (2002), molten salts method Gopalan Srikanth *et. al* (1996) and others. In spite of all these processes a high temperature sintering is required for the crystallization of $Bi_3Ti_4O_{12}$. Yang Qunbao *et. al.* (2003). Due to the presence of ferroelectric, piezoelectric properties, bismuth titanate is noted as a promising candidate in comparison to the lead zirconium titanate which is used primarily for non-volatile memory, piezoelectric applications. Absence of lead content in the composition of aurivillius structure makes bismuth titante an ecofriendly material system for versatile applications. Ng Hwee Szu *et. al.* (2002). High density, and proper microstructure are very essential to obtain such electrical properties Guha J.P. (1999). Solid state mix assisted mechano-chemical activation followed by annealings is used to synthesize Aurivillius Bismuth titanate as shown in this article. There is a limited research, so far, focusing on synthesis of the compound by such route which is a low cost easy method of synthesis without involvement of complex steps and precursors. The compound is analyzed for phase determination by XRD, morphology from FESEM, HRTEM bond formation from FTIR spectra along with band gap evaluation from UV-VIS spectra analysis.

2. EXPERIMENTAL

Stoichiometric amounts of bismuth oxide (Bi_2O_3) and titanium oxide (T_iO_2) AR Grade in 2:3 molar ratios were taken in an agate mortar for milling activation. Precursor powders were then mixed in the agate mortar-pestle. Solid state mixing was carried for eight hours followed by sintering at 1000°C for a 12 hour. soaking period in air atmosphere within a PID controlled furnace to synthesis bismuth titanate. The heating rate was fixed at 6°C per min, 5°C per min, 4°C per min for the range of 0°C to 600°C, 600°C to 800°C and lastly from 800°C to 1000°C for proper synthesis while using a normal cooling rate. The stoichometric equation to synthesize the required compound is given as $2Bi_2O_3 + 3TiO_2 = Bi_4Ti_3O_{12}$. The characterization techniques were analysed to determine the phases developed, morphological features, bonding and optical properties of the material. Using a wavelength of Cu Kα 1.54Å, 40mA, 50kV as current and voltage ratings within the scan range 2θ 10-80°, normal scan rate of 5°/min, crystallographic analysis of the sample was carried by XRD (Rigaku Ultima III) at ambient condition. M-O co-ordinations of the synthesized samples were identified by FTIR analysis (IR Prestige-21, Shimadzu) to obtain information for bonding in the sample. KBr powder was mixed with the sample to form a pellet under pressure of 6t/cm² for spectral analysis. To undergo morphological analyses of the samples using FESEM (Hitachi, S-4800) and HRTEM (JEOL, JEM 2100) operated at 200kV, conducting coating of gold was deposited (by sputtering) to avoid static charge accumulation in order to obtain a better resolution. Optical properties were determined from UV-VIS spectral analysis followed by band gap evaluation. The samples were prepared by sonication using high pure DI water as medium and put into a cuvette for analysis. Band gap calculation was carried using Tauc plot from UV-VIS spectra (Perkin Elmer, Lambda 35).

3. RESULTS AND DISCUSSION

Figure 1 shows the XRD patterns of the prepared nano-crystallites by modified solid state process. An XRD pattern indicates aurivillus Bismuth titanate formation as per JCPDS PDF # 802143. Thorough XRD pattern analysis indicates nil trace amount of bismuth oxide, titanium dioxide within the synthesized sample as residue or unreacted one. Major peaks for growth are observed along (-117) plane while other important peaks are observed at

(200), (111), (006), (0014). Growth of crystallites is possible when there is a thermodynamic feasibility of phases after proper nucleation along with development of such phases in preferred oriented planes. Thus, these observed planes or facets of planes indicate feasibility of the crystallite growth along these mentioned planes as observed from the aforementioned figures. None of the peaks, even in a minor form indicates phase decomposition or transition. Absence of precursor peaks or intermediate oxides in XRD spectra confirms purity of the Aurivillius phase. The crystallite sizes of the prepared sample is calculated using Scherrer's formula are expressed as $t = 0.9 \, \lambda / (\beta \cos \theta)$, where t is the particle size, λ is the X-ray wavelength, β is the line broadening at half of the maximum intensity in radians and θ is the Bragg angle in degree. Major peak (-117) is indexed for the crystallite size estimation. The indices observed are along either all odd or even (h, k, l) indices and such observations get matched with XRD analysis of Wang-Ming Chun *et. al.* (2008). The average particle size of BIT calculated from Scherrer's equation is around 65 nm. As observed, the peaks have are sharp narrow width, indicating high crystalline nature without any humps and deconvolution.

Spectral patterns of FTIR for the synthesized BIT are shown in Fig. 2 and they vary within the scan range from 400-4000 cm^{-1}. Molecular vibration bond for stretching vibrations, symmetric and asymmetric stretching condition is observed from FTIR spectra within the prescribed scan range. Major relevant bond formed for the respective Aurivillius phase related to M-O coordinations is observed to be within the range 400-700cm^{-1}. For synthesized material Bi-O bond vibration is observed to be about 500cm^{-1} while for Ti-O bond linkage is indicated by 1000 cm^{-1}. It is evident from Fig. 2 that for BIT formation distinct absorption intensity is around 500 cm^{-1}. Stretching vibrations of Bi–O bonds due to presence of absorption peak is strongly attributed to distorted BiO_6 octahedral units at around 490 cm^{-1} in the FTIR absorption spectra as reported by Rahaman Atiar *et. al.* (2016). The stretched band at around 632-700 cm^{-1} is due to Ti–O bond or TiO_4 tetrahedral Molla Rahaman Atiar *et. al.* (2016). The isosbestic point is observed at about 700 cm^{-1} which indicates that equilibrium exists between the oxide and bismuth containing species. Small absorbance spectra at around 470cm^{-1} is possibly due to O-Ti-O stretching vibration of TiO_2 which is used as precursor Liu Weiliang *et. al.* (2010).

Figure 3 indicates that the morphological features obtained from FESEM of synthesized Aurivillius type oxide after annealing at 1000ºC with a two hour soaking period. All morphological features observed for synthesized samples at different magnification and resolution exhibit agglomeration tendency while the growth pattern is more towards homogenous and uniform in nature. Sharp defined edges are noted for the plate type morphology of the particulates in all of the above. Multilayer, agglomerated, elongated structure is formed as a whole agglomerate of aurivillius BIT. Plates with elongated structured morphology are observed to be stacked together in some portions (Fig. 3-b) and top view of such stacked platelets (mulilayer) give rise to agglomerated form like irregular shape polygonal or regular polygonal (Fig. 3-a,d). Layer thickness of individual platelets is noted to be about 0.15µ. The experimental findings have some resemblance with morphological findings by Lin Xue *et. al.* (2012). They have worked on photocatalytic activity of bismuth titanate in presence of visible light after synthesis in the same way as by hydrothermal method. In those cases, microsphere with platelets are noted as morphology depending upon the concentration of $Ti(OC_4H_9)_4$ Lin Xue *et. al.* (2012). Similar results were also noted during hydrothermal synthesis of $Bi_4Ti_3O_{12}$. With increase in temperature regular plate shape also increases in number and the size also increases significantly Chen Zhiwu *et. al.* (2009). Negligible interconnected pores are noted amongst the agglomerated particulates. Agglomerate chunks are around 2.5µ while individual particulates are found to be around 0.02µ-0.075µ. The average size of a single particle, as determined from the FESEM micrographs, are in close correspondence to the particle sizes determined using the Scherrer's formula.

High resolution images of solid state synthesized aurivillius barium bismuth titanate are noted from HRTEM as shown in Fig. 4. BIT particles have strong agglomeration with elongated plate as shown throughout for HRTEM analysis. Both Figs. 4a) and Fig 4c) depict the elongated nature of platelets while Fig 4b) and Fig 4d) represent the sharp edges of an individual particulate. The elongated particulate has a width around 170nm and comprises of various small particulates. Both Figs. 4e) and 4f) represents agglomeration tendency as depicted from morphological analysis of FESEM studies. The agglomerated forms that have regular or irregular polygonal shapes are observed. The growth pattern of agglomerated form is homogenous in nature. Thus both FESEM and HRTEM analyses are found to be in correspondence with each other. Moreover, HRTEM studies confirm that particulates are in nano domain as observed from XRD crystallite size estimation by Scherrers formula. The agglomerated form varies from spherical to polygonal type morphology.

Figure 5 depicts the band gap of aurivillus bismuth titanate at 1000°C for 12 hours using Tauc plot. UV- VIS spectra are carried in the scan range of 200-850nm range in absorption mode. Powder samples are dispersed in alcohol after ultrasonication for one hour to prepare the samples for optical analysis. Tauc relation $(\alpha h v)^n = C(h v - E_g)$ is used where n =2, for direct allowed transition, n=1/2 for indirect allowed transition with the band structure.
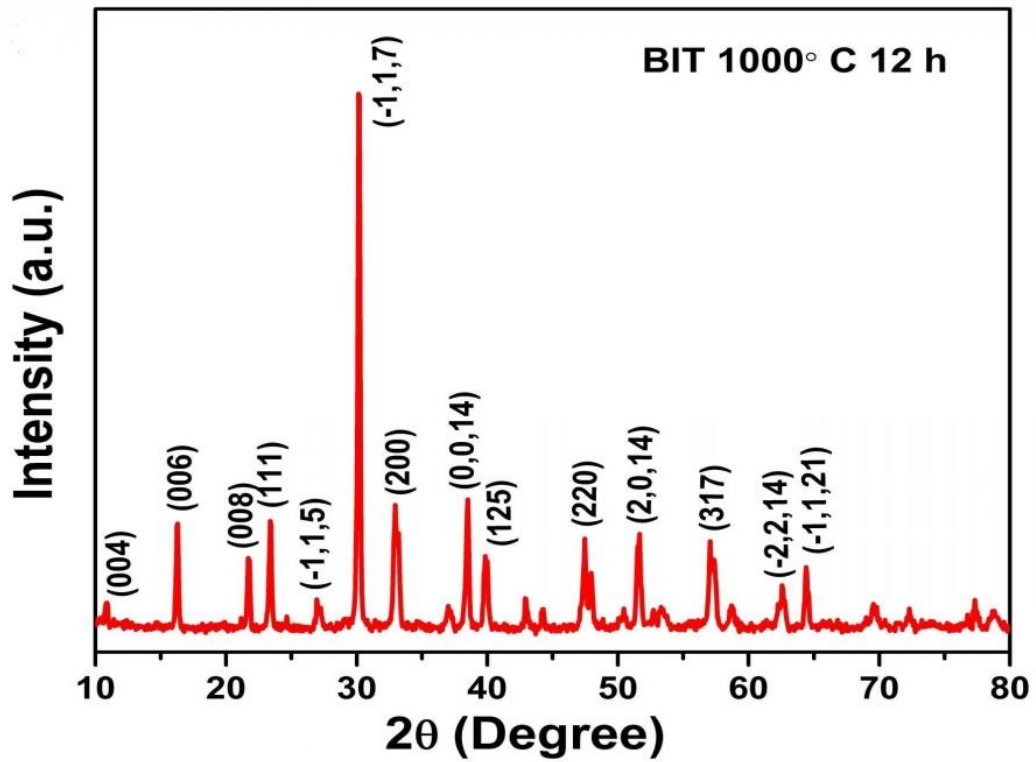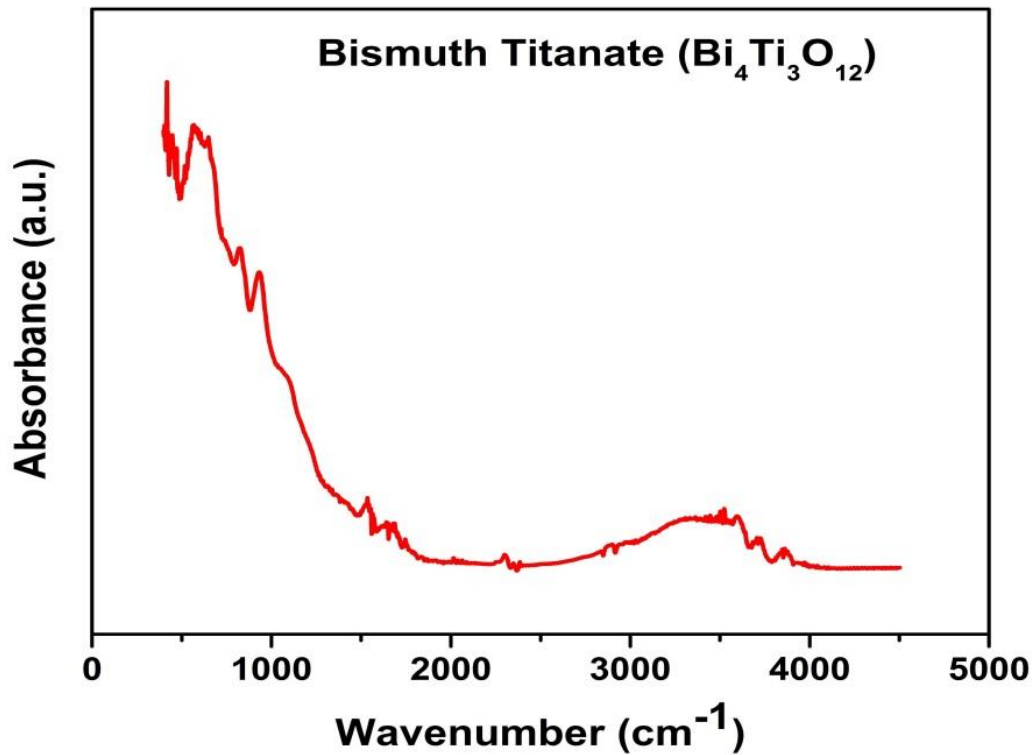
Figure 1. XRD of sintered Bismuth Titanate.

Figure 2. FTIR spectra of Aurivillius Bismuth Titanate sintered at 1200°C for 12 hours after 8 hours of milling activation.
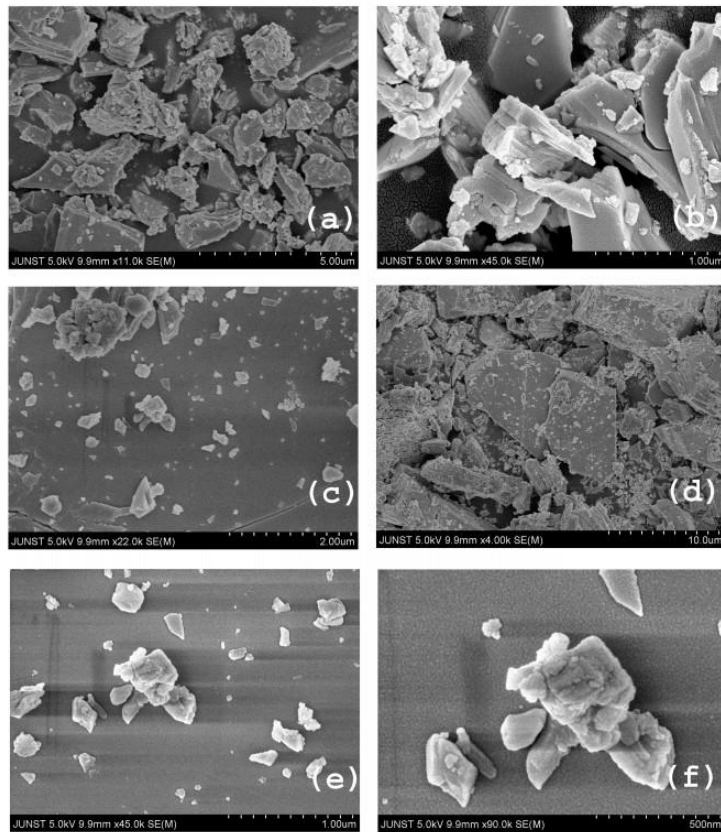
Figure 3. FESEM micrographs of bismuth titanate (BIT) sintered at 1000 °C for 12 hours.
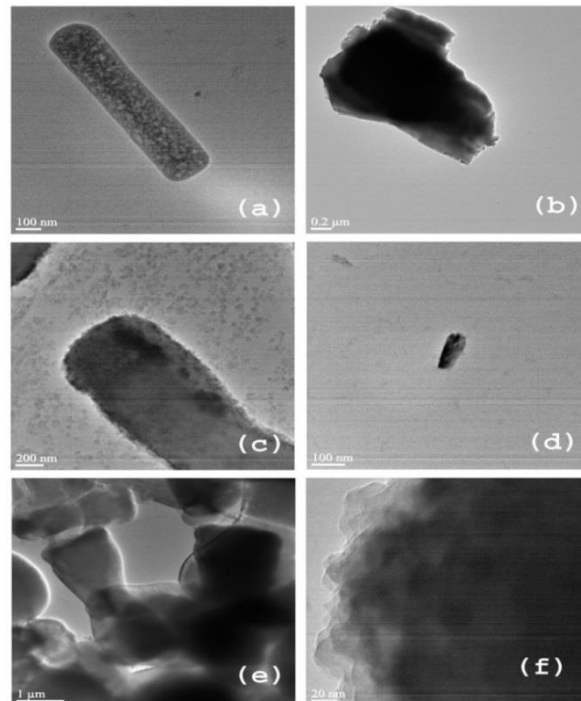

Figure 4. Typical HRTEM images of bismuth titanate (BIT) sintered at 1000°C for 12 hours.
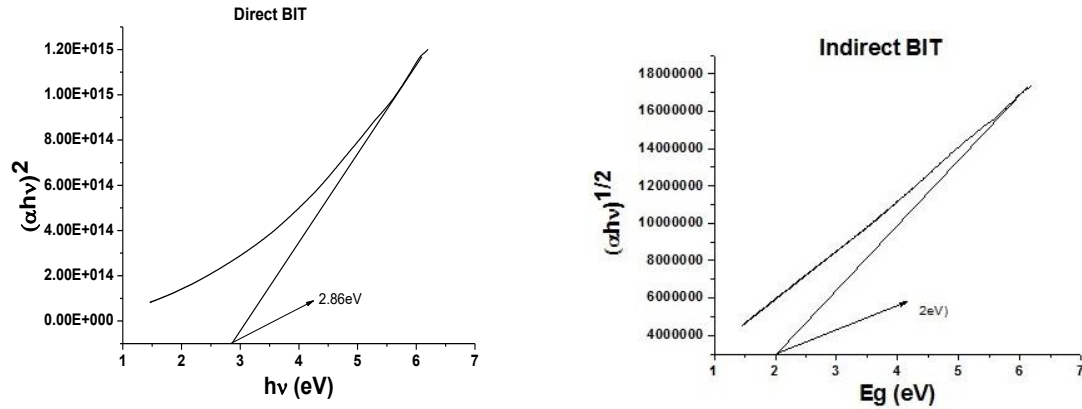
Figure 5. Direct and indirect band gap of Bismuth titanate by tauc plot at 1000°C for 12 hours.

Extrapolation of the tangent of the curve to the x-axis, gives the value of the sample's band gap. Direct and indirect band gap values of the synthesized sample are around 2.86eV and 2eV respectively. Hence, the Aurivillus sample is observed to be active for energy transition (electron transfer within the band structure) within the visible region. Thus, the synthesized material may have the possibility for photocatalytic applications, photo-induced devices in visible spectrum. Moreover, the band gap values are quite comparable with oxide semiconductors like zinc oxide, barium titanate, bismuth ferrite and others.

4. CONCLUSION

Bismuth titanate synthesis was carried after mechanochemical activation for eight hours along with annealing at 1000°C for 12 hrs. Aurivillius type structure with crystallite size around 65nm was confirmed from phase analysis by XRD. M-O coordination and the bonding confirm formation of bismuth titanate by FTIR analysis. Morphological studies from FESEM, HRTEM confirm agglomeration, elongated structure, polygonal regular or irregular type agglomerates with homogenous distribution. Agglomerates were around 2.5µ while individual particulates were around 0.02µ-0.075µ. Band gap values estimated that direct and indirect transitions were 2.86eV and 2eV respectively using tauc relation.

CONFLICT OF INTEREST

The authors declare no conflicts of interest.

FUNDING

REFERENCES

Chen Zhiwu, Yu Ying, HU Jianqiang, Shui Anze, HE Xinhua (2009), Hydrothermal synthesis and characterization of $Bi_4Ti_3O_{12}$ powders. *Journal of the Ceramic Society of Japan* 117(3): 264-267.

Gopalan Srikanth, Mehta Karun, Virkar V. Anil (1996), Synthesis of oxide perovskite solid solutions using the molten salt method. *Journal of Materials Research* 11(8): 1863–65.

Guha J.P. (1999), Reaction chemistry and sub solidus phase equilibria in lead-based relaxor systems: Part 1, formation and stability of the perovskite and pyrochlore compounds in the system PbO–MgO–Nb2O5. *Journal of Materials Science* 34(20): 4985–94.

HaoShuang Gu, Chen Peizhi, Zhou Youhua, Zhao Min, Kuang Anxiang, Li Xingjiao (1998), Reactions in preparing $Bi_4Ti_3O_{12}$ ultrafine powders by sol-gel process. *Ferroelectrics* 211: 271–280.

Horn A. Jeffrey, Zhang S C, Selvaraj U, Messing L. Gary, McKinstry-Trolier Susan (1999), Templated grain growth of textured bismuth titanate. *Journal of the American Ceramic Society* 82(4): 921–926.

Lin Xue, Lv Peng, Guan Qingfeng, Li Haibo, Zhai Hongjv, Liu Chunbo (2012), Bismuth titanate microspheres: Directed synthesis and their visible light photocatalytic activity. *Applied Surface Science* 258: 7146-7153.

Liu Weiliang, Wang Xinqiang, Tian Dong, Xiao Chenglong, Wei Zengjiang, Chen Shouhua (2010), Chemical reaction and crystalline procedure of bismuth titanate nanoparticles derived by metalorganic decomposition technique. *Materials Sciences and Applications* 1: 91-96.

Molla Rahaman Atiar, Tarafder Anal, Karmakar Basudeb (2016), Fabrication and properties of Nd^{3+}- doped ferroelectric barium bismuth titanate glass-ceramic nanocomposites. *Journal of Alloys and Compounds* 680: 237-246.

Ng Hwee Szu, Xue Junmin, Wang John (2002), Bismuth titanate from mechanical activation of a chemically coprecipitated precursor. *Journal of the American Ceramic Society* 85(11): 2660-2665.

Nogueira E. André, Longo Elson, Leite R. Edson, Camargo R. Emerson (2014), Synthesis and photocatalytic properties of bismuth titanate with different structures via oxidant peroxo method (OPM). *Journal of Colloid and Interface Science* 415: 89–94.

Osamu Y, Noboru M, Ken H (1991), Formation and characterization of alkoxy-derived $Bi_4Ti_3O_{12}$. *British Ceramic Transactions* 90: 111–113.

Pavlović Nikolina, Kancko Dejan, Szécsényi Mészáros Katalin, Srdić V. Vladimir (2009), Synthesis and characterization of Ce and La modified bismuth titanate. *Processing and Application of Ceramics* 3(1-2): 88-95.

Sedlar M, Sayer M (1996), Structural and electrical properties of ferroelectric bismuth titanate thin films prepared by the sol–gel method. *Ceramic International* 22(3): 241–247.

Shi Yanhui, Cao Changsheng, Feng Shouhua (2000), Hydrothermal synthesis and characterization of $Bi_4Ti_3O_{12}$. *Materials Letter* 46: 270–273.

Wang-Ming Chun, Wang Feng Jin (2008), Aurivillius phase potassium bismuth titanate: $K_{0.5}Bi_{4.5}Ti_4O_{15}$. *Journal of the American Ceramic Society* 91(3): 918-923.

Yang Qunbao, Li Yongxiang, Yin Qingrui, Wang Peiling, Cheng Bing-Yi (2003), $Bi_4Ti_3O_{12}$ nanoparticles prepared by hydrothermal synthesis. *Journal of the European Ceramic Society* 23: 161-166.